1-1-2009

Superconductivity in LaFeAs1-xPxO: effect of chemical pressures and bond covalency

Cao Wang
Zhejiang University, caow@uow.edu.au

Shuai Jiang
Zhejiang University

Qian Tao
Zhejiang University

Zhi Ren
Zhejiang University

Yuke Li
Zhejiang University

See next page for additional authors

A Letters Journal Exploring the Frontiers of Physics

May 2009

EPL, **86** (2009) 47002
doi: 10.1209/0295-5075/86/47002

www.epljournal.org

Superconductivity in $LaFeAs_{1-x}P_xO$: Effect of chemical pressures and bond covalency

Cao Wang[1], Shuai Jiang[1], Qian Tao[1], Zhi Ren[1], Yuke Li[1], Linjun Li[1], Chunmu Feng[2], Jianhui Dai[1], Guanghan Cao[1(a)] and Zhu-an Xu[1(b)]

[1] *Department of Physics, Zhejiang University - Hangzhou 310027, China*
[2] *Test and Analysis Center, Zhejiang University - Hangzhou 310027, China*

received 9 April 2009; accepted 27 April 2009
published online 26 May 2009

PACS 74.70.Dd – Ternary, quaternary, and multinary compounds (including Chevrel phases, borocarbides, etc.)
PACS 74.62.Bf – Effects of material synthesis, crystal structure, and chemical composition
PACS 74.62.Dh – Effects of crystal defects, doping and substitution

Abstract – We report the realization of superconductivity by an isovalent doping with phosphorus in LaFeAsO. X-ray diffraction shows that, with the partial substitution of P for As, the Fe_2As_2 layers are squeezed while the La_2O_2 layers are stretched along the *c*-axis. Electrical resistance and magnetization measurements show emergence of bulk superconductivity at ~ 10 K for the optimally doped $LaFeAs_{1-x}P_xO$ ($x = 0.25$–0.3). The upper critical field at zero temperature is estimated to be 27 T, much higher than that of the LaFePO superconductor. The occurrence of superconductivity is discussed in terms of chemical pressures and bond covalency.

Introduction. – Superconductivity can be induced by carrier doping in an insulator, semiconductor, and even metal. Representative examples are shown in hole-doped La_2CuO_4 [1], electron-doped $BaBiO_3$ [2], and electron-doped $TiSe_2$ [3]. Recently, superconductivity at 26 K was discovered in LaFeAsO by either electron doping with florine [4] or hole doping with strontium [5]. Subsequent replacements of La with other rare-earth elements raised the critical temperatures (T_c) over the McMillan limit (39 K) [6–8]. By electron doping with thorium in GdFeAsO, T_c has reached 56 K [9]. The discovery of high superconducting transition temperatures in these Fe-based compounds has generated great interest in the scientific community [10].

As a prototype parent compound of the new class of high-temperature superconductors, LaFeAsO crystallizes in ZrCuSiAs-type structure [11], which consists of insulating $[La_2O_2]^{2+}$ layers and conducting $[Fe_2As_2]^{2-}$ layers. In addition to the carrier doping in $[La_2O_2]^{2+}$ layers, partial substitution of Fe with Co [12,13] and Ni [14] also leads to superconductivity. Although the valence of the doped Co and Ni seems to remain 2+, electron carriers were believed to be induced owing to the itinerant character of the 3*d* electrons [13]. That is to say, the Fe-site substitution by Co/Ni still belongs to the scenario of carrier doping.

Apart from chemical doping, superconductivity was also observed via applying hydrostatic pressure in the parent compounds such as AFe_2As_2 ($A =$ Ca, Sr, Ba and Eu) [15–17] and LaFeAsO [18]. As "chemical pressures" may be produced by an isovalent substitution with smaller ions, we have tried the substitution of As by P in $EuFe_2As_2$ [19]. As a result, superconductivity appears below 26 K. Nevertheless, the superconductivity is then influenced by the subsequent ferromagnetic ordering of Eu^{2+} moments, and diamagnetic Meissner effect cannot be observed.

LaFeAsO is a prototype parent compound of ferroarsenide superconductors, showing spin-density-wave (SDW) antiferromagnetic ground state [20]. In contrast, the other end member $LaFeAs_{1-x}P_xO$ ($x = 1$) is a superconductor of ~ 4 K, showing non-magnetic behavior in the normal state [21]. According to a recent theory [22], partial substitution of P for As in the ferroarsenides may induce a quantum criticality, which could induce superconductivity. Therefore, the effect of P doping in LaFeAsO is of great interest. In this letter, we demonstrate bulk superconductivity in $LaFeAs_{1-x}P_xO$ at ~ 10 K with the evidences of both zero resistance and Meissner effect. This result establishes a stronger evidence

(a) E-mail: ghcao@zju.edu.cn
(b) E-mail: zhuan@zju.edu.cn

that "chemical pressures" and/or bond covalency may stabilize superconductivity in the ferroarsenide system.

Experimental. – $LaFeAs_{1-x}P_xO$ polycrystalline samples were synthesized by solid state reaction in vacuum using powders of LaAs, La_2O_3, FeAs, Fe_2As, FeP and Fe_2P. Similar to our previous report [13], LaAs, FeAs, Fe_2As, FeP and Fe_2P were presynthesized, respectively. La_2O_3 was dried by firing in air at 1173 K for 24 hours prior to using. All the starting materials are with high purity ($\geqslant 99.9\%$). The powders of these intermediate materials were weighed according to the stoichiometric ratios of $LaFeAs_{1-x}P_xO$ ($x = 0$, 0.1, 0.2, 0.25, 0.3, 0.35, 0.4, 0.5 and 0.6), thoroughly mixed in an agate mortar, and pressed into pellets under a pressure of 2000 kg/cm^2, operating in a glove box filled with high-purity argon. The pellets were sealed in evacuated quartz tubes, then heated uniformly at 1373 K for 40 hours, and finally furnace-cooled to room temperature.

Powder X-ray diffraction (XRD) was performed at room temperature using a D/Max-rA diffractometer with Cu-K_α radiation and a graphite monochromator. The detailed structural parameters were obtained by Rietveld refinements, using the step-scan XRD data with $10° \leqslant 2\theta \leqslant 120°$.

The electrical resistivity was measured using a standard four-terminal method. The measurements of magneto-resistance and Hall coefficient were carried out on a Quantum Design physical property measurement system (PPMS-9). The measurements of dc magnetic properties were performed on a Quantum Design Magnetic Property Measurement System (MPMS-5). Both the zero-field-cooling (ZFC) and field-cooling (FC) protocols were employed under the field of 10 Oe.

Results and discussion. – Figure 1 shows the XRD patterns for $LaFeAs_{1-x}P_xO$ samples. The sample of $x = 0$ shows single phase of LaFeAsO. With the P doping over 20%, small amount of Fe_2P impurity appears. When the doping level exceeds 50%, however, the impurity phase tends to disappear. The inset of fig. 1 plots the calculated lattice parameters as functions of nominal P content. Both a-axis and c-axis decrease with increasing x. Compared with the undoped LaFeAsO, a-axis decreases by 0.34% while c-axis shrinks by 0.87% for $LaFeAs_{0.7}P_{0.3}O$. Thus, the isovalent substitution of As with P indeed generates chemical pressure to the system. We note that the shrinkage in the basal planes is similar to that in $EuFe_2(As_{1-x}P_x)_2$, but the compression along c-axis is not as large as that in $EuFe_2(As_{1-x}P_x)_2$ [19].

The crystallographic parameters were obtained by the Rietveld refinement based on the ZrCuSiAs-type structure. An example of the refinement is seen in fig. 2. The reliability factor R_{wp} is 8.9% and the goodness of fit is 1.7, indicating fairly good refinement for the crystallographic parameters. Table 1 compares the structural data of the undoped and P-doped (by 30 at.%) samples. It is clear that As/P atoms are closer to the Fe planes

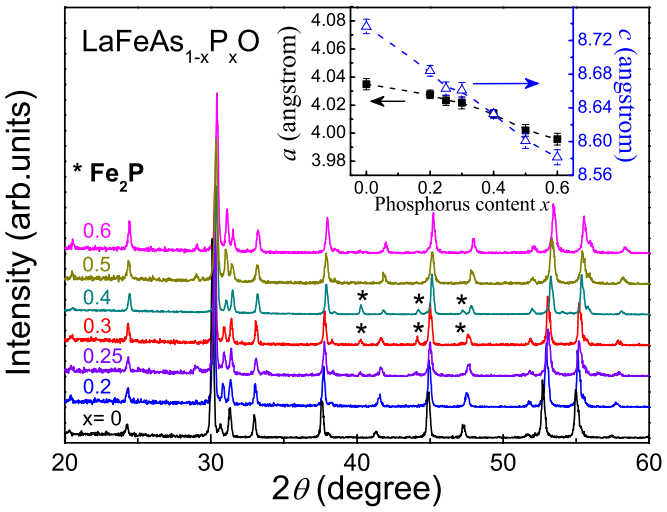

Fig. 1: (Colour on-line) X-ray powder diffraction patterns at room temperature for the $LaFeAs_{1-x}P_xO$ samples. Small amount of Fe_2P impurity is marked by asterisks. The inset plots the lattice parameters as functions of nominal phosphorus content.

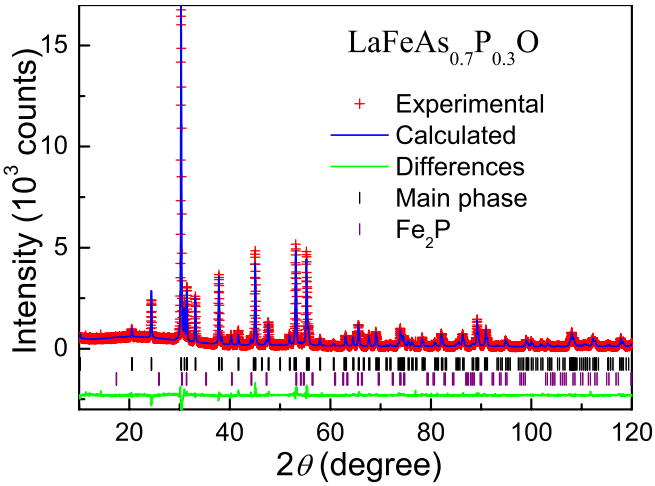

Fig. 2: (Colour on-line) An example of Rietveld refinement profile for $LaFeAs_{0.7}P_{0.3}O$. The Fe_2P impurity was included in the refinement.

for the P-doped compound, resulting in the flattening of the Fe_2As_2 layers. Interestingly, La atoms move toward the Fe_2As_2 layers, leading to the *increase* of the La_2O_2 layers. Thus the chemical pressure induced by the P doping actually causes compression in Fe_2As_2 layers, but stretching in La_2O_2 ones, along the c-axis. This explains why the decrease in c-axis in $LaFeAs_{1-x}P_xO$ is not as so much as that in $EuFe_2(As_{1-x}P_x)_2$. Besides, with the flattening of the Fe_2As_2 layers, the bond angle of As-Fe-As increases obviously. The large As-Fe-As angle may account for the relatively low T_c in $LaFeAs_{1-x}P_xO$ system (to be shown below), according to the empirical structural rule for T_c variations in ferroarsenides [23].

Table 1: Crystallographic data of $LaFeAs_{1-x}P_xO$ ($x = 0$ and 0.3) at room temperature. The space group is $P4/nmm$. The atomic coordinates are as follows: La (0.25,0.25,z); Fe (0.75,0.25,0.5); As/P (0.25,0.25,z); O (0.75,0.25,0).

Compounds	LaFeAsO	$LaFeAs_{0.7}P_{0.3}O$
a (Å)	4.0357(3)	4.0219(1)
c (Å)	8.7378(6)	8.6616(3)
V (Å^3)	142.31(2)	140.10(1)
z of La	0.1411(2)	0.1435(1)
z of As	0.6513(3)	0.6475(3)
La_2O_2 thickness (Å)	2.466(2)	2.486(1)
Fe_2As_2 thickness (Å)	2.644(2)	2.555(1)
Fe-Fe spacing (Å)	2.8536(3)	2.8439(1)
As-Fe-As angle (°)	113.5(1)	115.1(1)

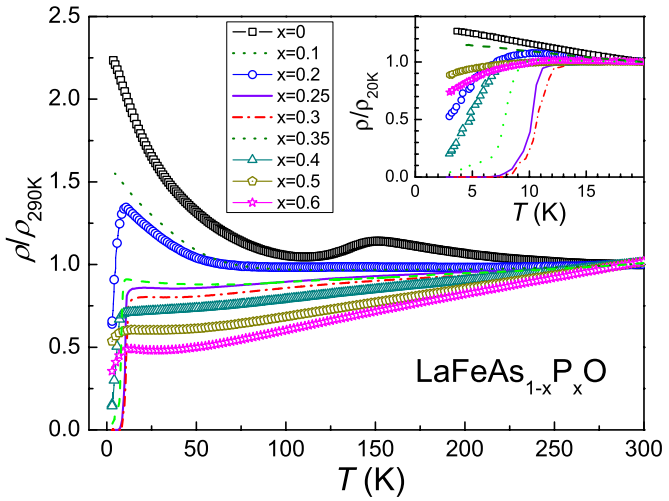

Fig. 3: (Colour on-line) Temperature dependence of resistivity for $LaFeAs_{1-x}P_xO$ samples. The inset shows an expanded plot. The data are normalized for comparison.

The temperature dependence of resistivity (ρ) for $LaFeAs_{1-x}P_xO$ samples is shown in fig. 3. The ρ of the undoped LaFeAsO shows anomaly at 150 K, where a structural phase transition takes place [20]. On doping 10% P, the anomaly is hard to see and ρ exhibits semiconducting behavior below 100 K. For $x = 0.2$, ρ is found to decrease quickly below 7 K, suggesting a superconducting transition though zero resistance is not achieved down to 3 K. For $x = 0.25$ and 0.3, ρ drops sharply at ~ 11 K, and the midpoint superconducting transition temperatures T_c^{mid} are 10.3 K and 10.8 K, respectively. With further increasing x to 0.4, T_c^{mid} decreases to 5 K, and the superconducting transition becomes broadened. For $x = 0.5$ and 0.6, only kinks are shown below 10 K in the $\rho(T)$ curves, suggesting that the superconducting phase has a very small fraction.

Superconductivity in $LaFeAs_{1-x}P_xO$ is confirmed by the dc magnetic susceptibility (χ) measurements, shown

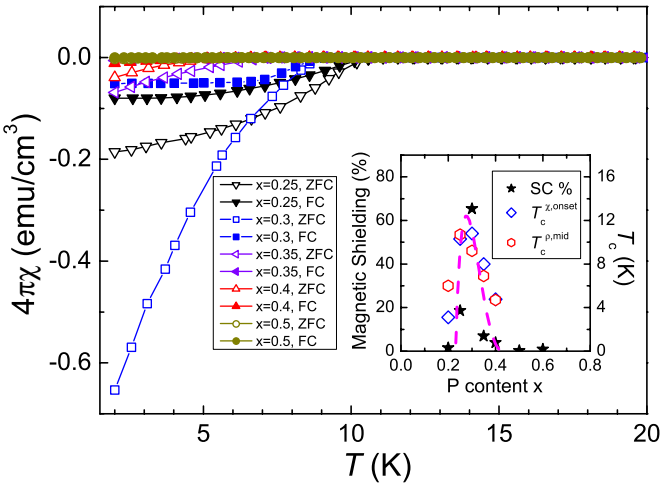

Fig. 4: (Colour on-line) Temperature dependence of dc magnetic susceptibility of $LaFeAs_{1-x}P_xO$ ($0.25 \leqslant x \leqslant 0.6$) samples. The applied field is 10 Oe. Note that the background signals due to ferromagnetic Fe_2P impurity was deducted to show the superconducting transitions clearly. The inset shows the superconducting transition temperature and the superconducting magnetic shielding percentage as functions of doping level x.

in fig. 4. After deducting the magnetic background signals of the ferromagnetic Fe_2P impurity, diamagnetic transitions are obvious for the superconducting samples. Strong diamagnetic signals can be seen below 11 K for samples of $x = 0.25$ and 0.3 in both ZFC and FC data. The volume fraction of magnetic shielding (ZFC) at 2 K achieves 65% for $x = 0.3$, indicating bulk superconductivity. For the samples of $x = 0.2$ and 0.4, however, the magnetic shielding fraction at 2 K is less than 2% and 5%, respectively, suggesting inhomogeneity of the P doping for these two samples. The samples of $x = 0.5$ and 0.6 only show trace and broad diamagnetic signals, consistent with the kinks in the above resistivity measurements. Thus one would expect non-superconductivity for a uniform samples of $x \leqslant 0.2$ and $x \geqslant 0.4$. The superconducting phase diagram is depicted in the inset of fig. 4. A dome-like $T_c(x)$ curve is displayed.

Figure 5 shows the temperature dependence of resistivity under magnetic fields for $LaFeAs_{0.7}P_{0.3}O$. As expected, the resistive transition shifts towards lower temperature with increasing magnetic fields. The broad transition tails under magnetic fields are probably due to the superconducting weak links in grain boundaries as well as the vortex motion. Thus, we define $T_c(H)$ as a temperature where the resistivity falls to 90% of the normal-state value. The initial slope $\mu_0 \mathrm{d}H_{c2}/\mathrm{d}T$ near T_c is -3.59 T/K, as shown in the inset of fig. 5. The upper critical field $\mu_0 H_{c2}(0)$ is then estimated to be ~ 27 T by using the Werthamer-Helfand-Hohenberg (WHH) relation, $H_{c2}(0) \approx 0.691 |\mathrm{d}H_{c2}/\mathrm{d}T| T_c$ [24]. The value of $\mu_0 H_{c2}(0)$ exceeds the Pauli paramagnetic limit [25] ($H_P(0) \approx 1.84 T_c$ tesla for an isotropic s-wave spin-singlet

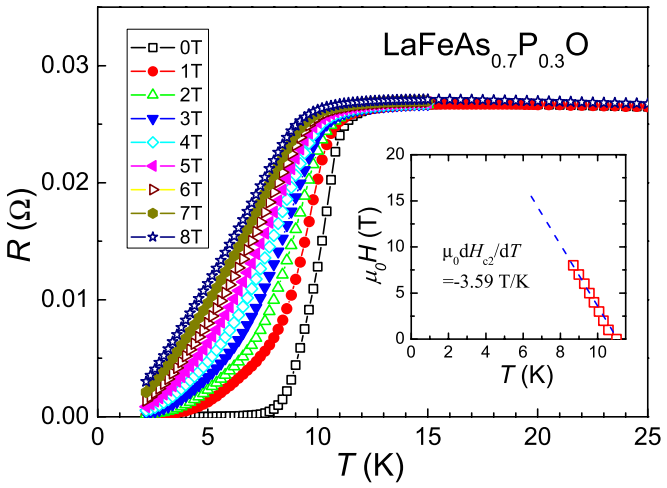

Fig. 5: (Colour on-line) Temperature dependence of the electrical resistance of the $LaFeAs_{0.7}P_{0.3}O$ sample around T_c in fixed applied magnetic fields. The inset shows the temperature dependence of the upper critical magnetic fields.

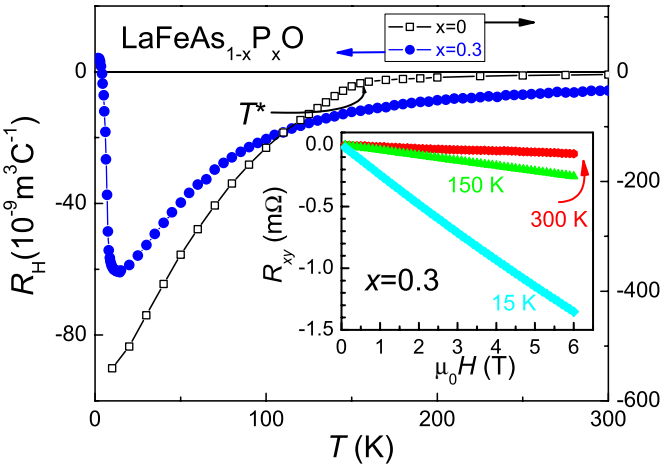

Fig. 6: (Colour on-line) Temperature dependence of Hall coefficient for the superconductor $LaFeAs_{0.7}P_{0.3}O$, in comparison with that of the parent compound LaFeAsO. The inset shows the field dependence of the Hall resistance at several fixed temperatures.

superconductor) by 35%. Similar observations have been reported in $LaFeAsO_{1-x}F_x$ [26] and $LaFe_{1-x}Ni_xAsO$ [14] systems. The upper critical field of LaFePO is far below its Pauli paramagnetic limit [27], revealing the difference between LaFePO and $LaFeAs_{0.7}P_{0.3}O$ superconductors.

Figure 6 shows that the Hall coefficient (R_H) of $LaFeAs_{0.7}P_{0.3}O$ is negative in the normal state, suggesting the dominant charge transport by the electron conduction. The normal state $R_H(T)$ exhibits very strong temperature dependence (especially at low temperatures), compared with the $LaFeAsO_{1-x}F_x$ superconductors [28,29]. This indicates that the multiband effect is more significant in the P-doped superconductors. The room temperature R_H value is $-5.7 \times 10^{-9}\,\mathrm{m^3\,C^{-1}}$, very close to that of the undoped LaFeAsO ($-4.8 \times 10^{-9}\,\mathrm{m^3\,C^{-1}}$), supporting that the P doping does not induce extra charge carriers. Below 10 K, $|R_H|$ decreases very sharply, consistent with the superconducting transition. The non-zero $|R_H|$ is due to the non-zero resistance under high magnetic fields. The $|R_H|$ of undoped LaFeAsO increases rapidly below $T^* \sim 155$ K because of the structural phase transition and the subsequent SDW ordering [28]. Such a transition cannot be detected in $LaFeAs_{0.7}P_{0.3}O$. Since the P doping does not change the number of Fe 3*d* electrons, the severe suppression of SDW order by P doping suggests that Fermi surface nesting is unlikely to account for the SDW ordering in the LaFeAsO.

Now, let us discuss the occurrence of superconductivity in P-doped LaFeAsO. While the chemical-pressure-induced superconductivity in P-doped LaFeAsO basically agrees with the static-pressure–induced superconductivity in LaFeAsO [18], there is difference between the two kinds of pressure. The hydrostatic pressure generally produces a homogeneous effect, but chemical pressure may be selective to a particular structural unit in a complex compound. In the present $LaFeAs_{1-x}P_xO$ system, P doping leads to the squeezing (stretching) in Fe_2As_2 (La_2O_2) layers, respectively, along the *c*-axis. Band calculations [30] suggest that the relative positions of As/P to Fe planes affect the electronic structure. When arsenic is moved closer to the iron planes, the two-dimensional pocket with d_{xy} character in the LaFeAsO evolves into a three-dimensional pocket with $d_{3z^2-r^2}$ character. This might correlate with the three-dimensional superconductivity in the two-dimensional system [31]. Thus, the appearance of superconductivity in P-doped LaFeAsO suggests that the $d_{3z^2-r^2}$ band should be important for superconductivity. It is noted that the La-site replacement with smaller rare-earth elements, which also produce chemical pressures, influences little on the SDW order, and induces no superconductivty [32]. A possible reason is that the chemical pressure is applied mainly in La_2O_2 rather than Fe_2As_2 layers.

In addition to the above structural points of view, the difference in covalency for the bonding of Fe-As/P may also play a role for superconductivity. The P substitution for As in the undoped iron pnictides was proposed as a means to access the magnetic quantum criticality in an unmasked fashion [22]. The narrow superconducting region in $LaFeAs_{1-x}P_xO$ supports the scenario of quantum criticality with magnetic fluctuations for the superconducting mechanism. Nevertheless, much work is needed to address this issue.

In summary, we have discovered bulk superconductivity in $LaFeAs_{1-x}P_xO$ by the isovalent substitution of As with P. Superconductivity emerges in the region of $0.2 < x < 0.4$ with the maximum T_c of 10.8 K. Unlike previous doping strategy in LaFeAsO, the P doping does not change the number of Fe 3*d* electrons. This chemical-pressure–induced superconductivity in ferroarsenides contrasts sharply with

the case in cuprates, where superconductivity is always induced by doping of charge carriers into an AFM Mott insulator. We suggest that both the chemical pressure (applied selectively to the Fe_2As_2 layers) and the covalency of Fe-P bonding may lead to quantum criticality, facilitating superconductivity.

* * *

This work is supported by the NSF of China (Contract Nos. 10674119 and 10634030), the National Basic Research Program of China (Contract No. 2007CB925001) and the PCSIRT of the Ministry of Education of China (IRT0754).

REFERENCES

[1] Bednorz J. G. and Muller K. A., *Z. Phys. B*, **64** (1986) 189.
[2] Cava R. J. *et al.*, *Nature*, **332** (1988) 814.
[3] Morosan E. *et al.*, *Nat. Phys.*, **2** (2006) 544.
[4] Kamihara Y. *et al.*, *J. Am. Chem. Soc.*, **130** (2008) 3296.
[5] Wen H. H. *et al.*, *EPL*, **82** (2008) 17009.
[6] Chen X. H. *et al.*, *Nature*, **453** (2008) 761.
[7] Chen G. F. *et al.*, *Phys. Rev. Lett.*, **100** (2008) 247002.
[8] Ren Z. A. *et al.*, *EPL*, **83** (2008) 17002.
[9] Wang C. *et al.*, *EPL*, **83** (2008) 67006.
[10] Johannes M., *Physics*, **1** (2008) 28.
[11] Quebe P. *et al.*, *J. Alloys Compd.*, **302** (2000) 70.
[12] Sefat A. S. *et al.*, *Phys. Rev. B*, **78** (2008) 104505.
[13] Wang C. *et al.*, *Phys. Rev. B*, **79** (2009) 054521.
[14] Cao G. H. *et al.*, *Phys. Rev. B*, **79** (2009) 174505.
[15] Torikachvili M. S. *et al.*, *Phys. Rev. Lett.*, **101** (2008) 057006; Park T. *et al.*, *J. Phys.: Condens. Matter*, **20** (2008) 322204.
[16] Alireza P. L. *et al.*, *J. Phys.: Condens. Matter*, **21** (2009) 012208.
[17] Miclea C. F. *et al.*, arXiv:0808.2026 (2008).
[18] Okada H. *et al.*, *J. Phys. Soc. Jpn.*, **77** (2008) 113712.
[19] Ren Z. *et al.*, *Phys. Rev. Lett.*, **102** (2009) 137002.
[20] Cruz C. *et al.*, *Nature*, **453** (2008) 899.
[21] Kamihara Y. *et al.*, *J. Am. Chem. Soc.*, **128** (2006) 10012.
[22] Dai J. H. *et al.*, *Proc. Natl. Acad. Sci. U.S.A.*, **106** (2009) 4118.
[23] Zhao J. *et al.*, *Nat. Mater.*, **7** (2008) 953; Lee C. H. *et al.*, *J. Phys. Soc. Jpn.*, **77** (2008) 083704.
[24] Werthamer N. R., Helfand G. and Hohenberg P., *Phys. Rev.*, **147** (1966) 295.
[25] Clogston A. M., *Phys. Rev. Lett.*, **9** (1962) 266; Chandrasekhar B. S., *Appl. Rev. Lett.*, **1** (1962) 7.
[26] Fuchs G. *et al.*, *Phys. Rev. Lett.*, **101** (2008) 237003.
[27] Hamlin J. J. *et al.*, *J. Phys.: Condens. Matter*, **20** (2008) 365220.
[28] Sefat A. S. *et al.*, *Phys. Rev. B*, **77** (2008) 174503; MacGuire M. A. *et al.*, *Phys. Rev. B*, **77** (2008) 094517.
[29] Zhu Z. W. *et al.*, *New J. Phys.*, **10** (2008) 063021.
[30] Vildosola V. *et al.*, *Phys. Rev. B*, **78** (2008) 064518.
[31] Yuan H. Q. *et al.*, *Nature*, **457** (2009) 565.
[32] McGuire M. A. *et al.*, *New J. Phys.*, **11** (2009) 025011.